J. Mod. Transport. (2014) 22(1):59–63
DOI 10.1007/s40534-014-0037-z

www.springer.com/40534

The preparation process and feature of the topological insulator Bi_2Te_3

Peng Chen · Dajin Zhou · Pingyuan Li · Yajing Cui · Yongliang Chen

Received: 31 October 2013 / Revised: 16 January 2014 / Accepted: 18 January 2014 / Published online: 9 February 2014

Abstract Topological insulators are insulating in the bulk but have metallic surface states. Its unique physicochemical properties can find numerous applications in electronics, spintronics, photonics, the energy sciences, and the signal control of transportation. We report an experimental approach to synthesize the high-quality single crystal of topological insulator Bi_2Te_3 by using self-flux method. We obtained the optimal preparation conditions by adjusting the parameters of heat treatment, and successfully prepared the single-crystal Bi_2Te_3 sample. The as-grown samples have a surface with bright metallic luster and are soft and fragile. Furthermore, Bi_2Te_3 has the obvious layer structure from SEM results. The data of X-ray diffraction and scanning electron microscope show that Bi_2Te_3 single crystal grows along the *c*-axis with the order of $Te^{(1)}$–Bi–$Te^{(2)}$–Bi–$Te^{(1)}$ and crystallizes in the hexagonal system with space group of R/3 m. The ρ–T curve shows that ρ decreases with temperature, showing metallic behavior over the whole temperature range.

Keywords Bi_2Te_3 · Single crystal · Topological insulator

1 Introduction

Topological insulators (TIs) are a new class of quantum states of matter with topologically protected conducting surface states, arising from the topology of the bulk electronic band structure [1–3]. They are insulating in the bulk but possess metallic surface states protected by time-reversal symmetry [4]. The surface structure is composed of single Dirac cones, and belongs to the Dirac particles system [5]. The carrier can be transmitted in the surface without scattering and energy loss. The topological surface states are gapless, and ambipolar conduction in the gate voltage tuned devices is taken as a signature of TI surface transport [6]. Because of these features, TI materials have great application prospects in the field of transistors, storage devices, magnetic sensors, and energy efficient products. Three-dimensional TIs including Sb_2Te_3, Bi_2Se_3, and Bi_2Te_3 are also excellent thermoelectrics, which have been intensively investigated for optimized thermoelectric performance in the recent decades [7, 8]. The theories and experiments have successively confirmed that they have large bulk band gap and single Dirac cone surface states [9–12]. They have quickly become a hot spot in the study of topological insulator material. The topological characteristic of Bi_2Te_3 was predicted by first-principles calculation and analysis of the model in Ref. [10] and observed by the angle-resolved photoemission spectroscopy (ARPES) [12, 13]. The Fermi surface (FS) is the shape of the snowflake-like. The Bi_2Te_3 single crystal was predicted to be a bulk insulator, and the electron carriers were observed in experiment to arise from crystal imperfections, specifically vacancies and defects [12]. It is found that increasing Se concentration effectively suppresses the bulk carrier transport and induces semiconducting behavior in $Bi_2(Te_{1-x}Se_x)_3$. An ambipolar field effect from the gapless surface states was observed in $Bi_2(Se_{0.8}Te_{0.2})_3$ [14].

The single crystal along the *c*-axis with $Te^{(1)}$–Bi–$Te^{(2)}$–Bi–$Te^{(1)}$ cycle stacked growth, belongs to the hexagonal

P. Chen · D. Zhou · P. Li · Y. Cui · Y. Chen (✉)
Key Laboratory of Magnetic Levitation Technologies and Maglev Trains, Ministry of Education of China, and Superconductivity and New Energy R&D Center, Southwest Jiaotong University, Chengdu 610031, China
e-mail: llchen@home.swjtu.edu.cn

system, and space group is R/3 m. Between Te and Bi layer is a covalent bond, and Van-der Waals bond between Te and Te layer. So the single Bi_2Te_3 is cleavage easily along the basal plane. Near the melting point temperature Bi_2Te_3 deviates from the strict ratio of chemical components. It presents a little excess Bi that Bi accounted for 40.065 % of atomic weight ratio and Te accounted for 59.935 % [15].

Bi_2Te_3 can greatly improve the speed of computer chips and efficiency. Using existing semiconductor technology, this kind of material can allow electrons to move on the surface without energy consumption at room temperature, so the application of this chip to modern transportation will lead to a leap.

Early by directional solidification method and the method of zone melting method prepared Bi_2Te_3 single crystal or columnar crystals; commercial production is also using these methods. Bi_2Te_3 as thermoelectric material was prepared by hot pressing method [16], the SPS (spark plasma sintering) method [17], hot extrusion method [18], solvent method [19], and so on. The samples with irregular polyhedron did not show the structural characteristics and contained an impurity phase [15]. Recently, the topological property of Bi_2Te_3 has been confirmed [12, 13]. In order to better study the bizarre properties of the TIs, we need the high-quality single-crystal material. So we have done many times trials according to the structure characteristics of Bi_2Te_3 single crystal with the self-flux method. To try and improve the process of proportioning, sample preparation, sintering, testing, etc., we summarize an optimization method of preparation of Bi_2Te_3 single crystal of high-quality material.

2 Experimental

High-purity elemental Bi (99.999 %) and Te (99.999 %) were used for the Bi_2Te_3 crystal growth. Bi and Te mixed with a molar ratio of 2:3 were fully grinded in glove box filled with argon at least 2 h, enclosed into evacuated quartz tubes, and then in heat treatment with the process of Fig. 1. We design three groups of Bi_2Te_3 samples (see Table 1). The first group (H-750–H-850) is to change the highest temperature in the range of 750–850 °C, and keep heating time, quenching temperature, cooling rate unchanged; the second group (Q500–Q580) is to change quenching temperature from 500 to 580 °C, and keep other conditions unchanged; the third group(C-4–C-6) is only to change cooling rate.

The crystal structure was studied by powder X-ray diffraction (XRD) using an X'Pert MRD diffractometer with Cu $K\alpha$ radiation. All observed reflections were indexed.

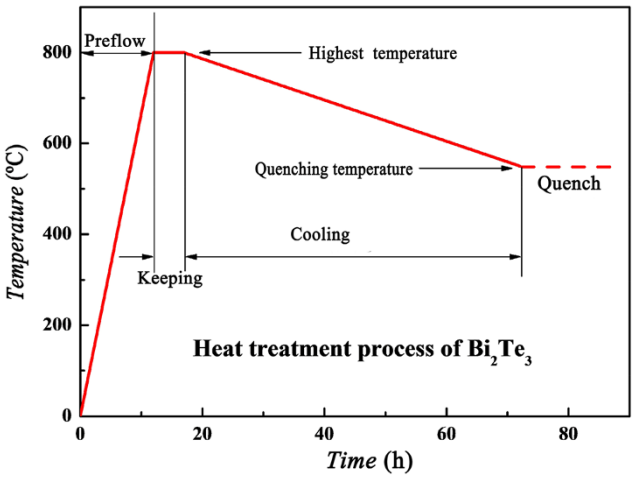

Fig. 1 Heat treatment process of Bi_2Te_3

Table 1 The grouped control variables in the heat treatment process (*H* highest, *Q* Quenching, and *C* Cooling)

No.	Highest temperature (°C)	Keeping time (h)	Quenching temperature (°C)	Cooling rate (°C/h)
H-750	**750**	5	550	5
H-780	**780**	5	550	5
H-800	**800**	5	550	5
H-820	**820**	5	550	5
H-850	**850**	5	550	5
Q-500	800	5	**500**	5
Q-550	800	5	**550**	5
Q-560	800	5	**560**	5
Q-570	800	5	**570**	5
Q-580	800	5	**580**	5
C-4	800	5	550	**4**
C-5	800	5	550	**5**
C-6	800	5	550	**6**

Bold values indicate differences of the heat treatment processes

Lattice constants were determined from LeBail refinements. Microstructure and composition of the sample were analyzed using a field emission scanning electron microscope (FESEM) equipped with an energy dispersive X-ray analysis (EDX). Resistivity measurements were performed with a physical property measurement system (PPMS, Quantum Design).

3 Results and discussions

Figure 2a, c, e show the XRD data for all the samples. Most of XRD peaks correspond to (00*L*) reflections, (006),

(0015), (0018), and (0021) distributed in the about 17.5°, 44.5°, 54.5°, and 64.5°, respectively. Calculating the cell parameters of every sample based on each of the main peak of sample, we draw out the curve of cell parameters c with temperature (see Fig. 2b, d, f). Bi_2Te_3 single crystal grows along the c-axis, so we only consider the value of the c. Figure 2b, d show that the value of c increases gradually with the highest temperature and the quenching temperature gradually; Fig. 2f shows that c value decreases with the increase of cooling rate.

According to the standard PDF card, we can know that the Bi_2Te_3 lattice parameters are $a = b = 4.3852$ and $c = 30.4830$ Å [20]. In Fig. 2b, d, f, $c = 30.48$ Å corresponds to the highest temperature 810 °C, quenching temperature 560 °C, and the cooling rate 4.4 °C/h.

We have got the sample of Bi_2Te_3 with the highest temperature 810 °C, quenching temperature 560 °C, and the cooling rate 4.4 °C/h. Figure 3 shows XRD pattern of the powder and single crystal as-grown samples Bi_2Te_3. After the Bi_2Te_3 standard pattern contrast, the vast majority

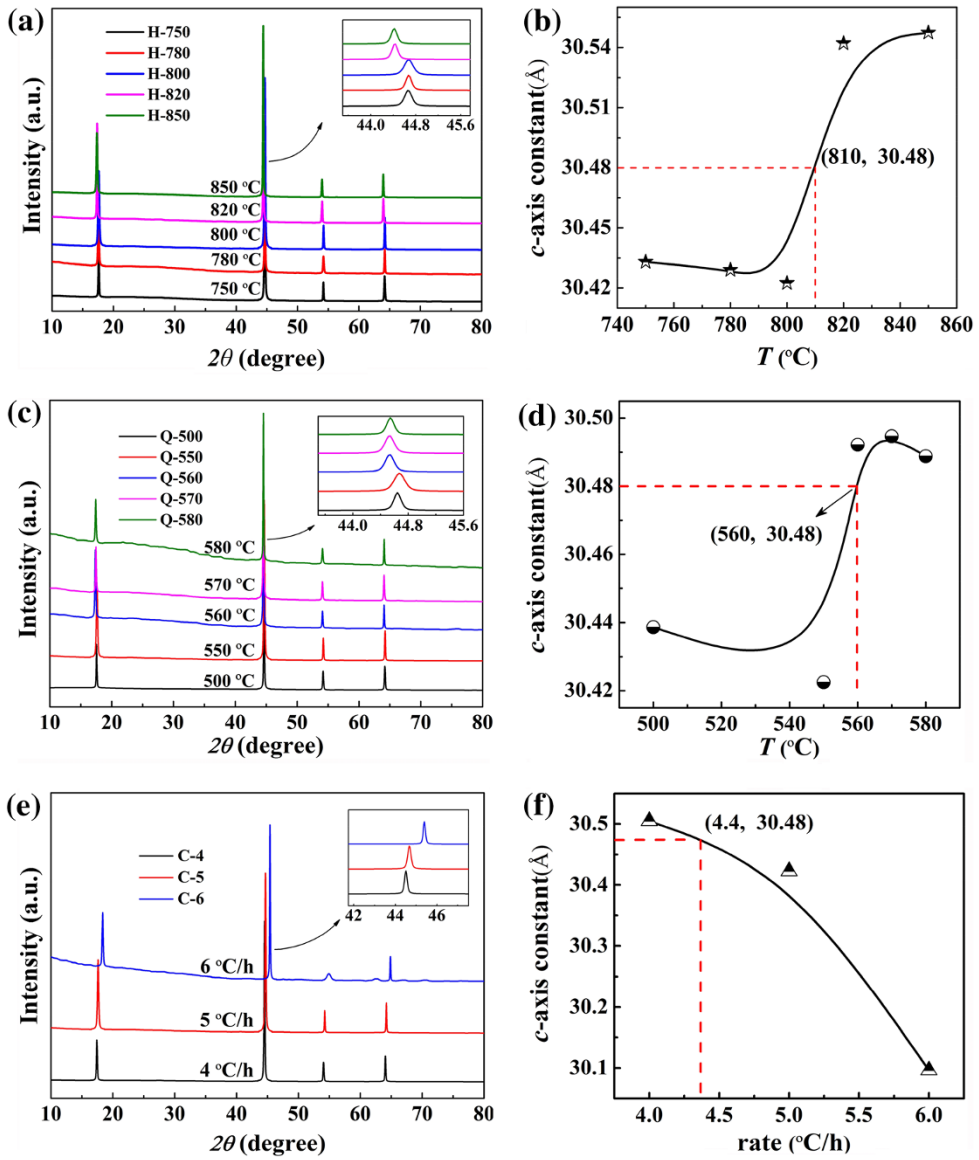

Fig. 2 X-ray diffraction curves of the H-750–H-850 (**a**), Q-500–Q-580 (**c**), and C-4–C-6 (**e**) and curves of cell parameters c with the highest temperature (**b**), quenching temperature (**d**), and cooling rate (**f**)

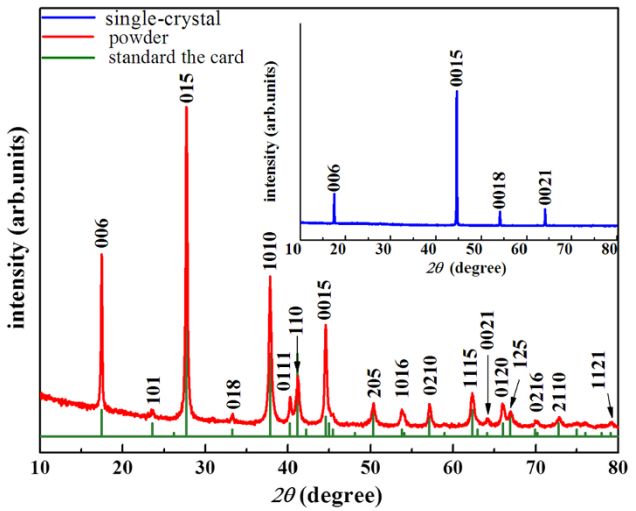

Fig. 3 Bi_2Te_3 powder X-ray diffraction pattern, inset is single crystal X-ray diffraction pattern

Table 2 Five strong peaks value with its corresponding interplanar distance *d*

Peak	006	015	1,010	110	0,015
d	5.07422	3.22059	2.37772	2.19265	2.03361

of the main peak marked in the picture can better match with standard pattern, indicating that the high-purity Bi_2Te_3 sample was obtained. The single-crystal sample only has (00*L*) peaks (*L* is 3*n*). It grows along the *c*-axis with the order of $Te^{(1)}$–Bi–$Te^{(2)}$–Bi–$Te^{(1)}$ and crystallizes in the hexagonal system with space group of R/3 m. We calculated lattice parameters by taking the five strong peaks' interplanar distances *d* (Table 2) from the XRD pattern of Bi_2Te_3 powder. The lattice parameters are $a = b = 4.38456$ and $c = 30.50063$ Å, which are consistent basically with the standard PDF card ($a = b = 4.3852$ and $c = 30.4830$ Å). However, the *c* values of the samples H-800 and Q-550 are 30.42248 and 30.42369 Å, respectively, which have large difference with standard values.

It can be seen from Fig. 4a that the sample surface has a bright metallic luster; there is an obvious hierarchical structure, and the surface is relatively flat. Figure 4b is EDX spectrum picture of Bi_2Te_3, Bi(L) and Te (M) in weight percentage of 52.82 % and 47.18 %, and the atomic percentage of 40.61 % and 59.39 %, respectively. In this sample, the atom ratio of Bi and Te was close to 2:3, Bi slightly excess. These results also deviated in component the stoichiometric ratio. It is consistent with the Bi–Te alloy phase diagram.

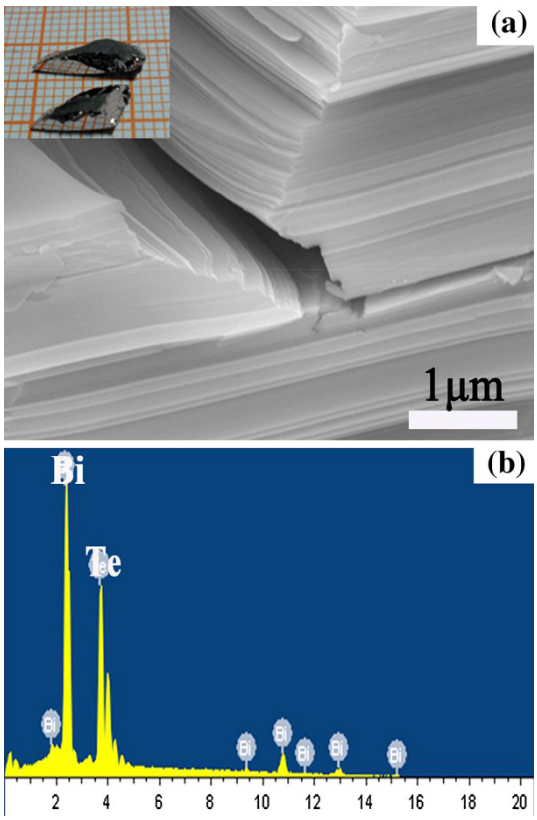

Fig. 4 SEM photographs of the single crystal of Bi_2Te_3 in 25,000 times and inset shows its physical picture. The conditions are that the highest temperature is 810 °C, quenching temperature is 560 °C, and the cooling rate is 4.4 °C/h (**a**) and EDX spectrum picture of the Bi_2Te_3 single crystal (**b**)

Figure 5a shows the resistance dependence of temperature curve of the Bi_2Te_3 with the magnetic field parallel to the *c*-axis, and it can be seen that the sample shows metallic behavior over the whole temperature range. The values of resistances increase gradually with the temperature and the intensity of the applied magnetic field. The entire curves have the same variation trend. We did not observe any induced insulators conduction or abnormal behavior due to the additional magnetic field. The tiny fluctuation of the resistance is found near 50 K. Figure 5b is the curve of the resistances dependence of the magnetic field parallel to the *c*-axis at $T = 5$ K. The values of resistances increase gradually with the applied magnetic field. At the high field, the curve of *R* versus *H* is linear. However, it deviates from the straight line at the part of the low filed. The linear variation law of the magnetic resistance may be associated with the surface state of TI. At low field the magnetic resistance deviates from the linearity, which may be associated with the weak anti-localization (WAL).

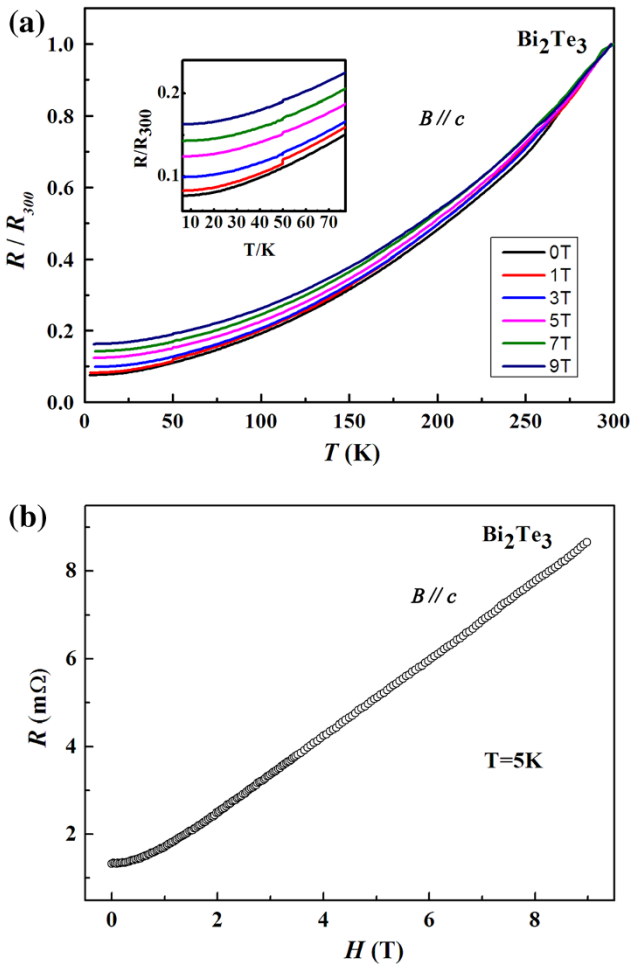

Fig. 5 **a** The *R–T* curve (0–9 T) of the Bi_2Te_3. The resistances at 300 K are 0.14331, 0.14224, 0.14527, 0.14495, 0.14729, and 0.14737 Ω, respectively. **b** The *R–H* curve ($T = 5$ K) of the Bi_2Te_3

4 Conclusions

We prepared the high-quality single-crystal synthesis of TI Bi_2Te_3 with the self-flux method. By controlling single variable and adjusting the parameters of heat treatment, we determined the optimal conditions for the highest temperature 810 °C, the quenching temperature 560 °C, and the cooling rate 4.4 °C/h. Bi_2Te_3 single crystal prepared under this condition has smooth surface with bright metallic luster and obvious layered structure, showing metallic behavior over the temperature range 7–300 K. At low temperature, the resistance increases as additional magnetic field increase, and shows linear magnetic resistance behavior in the high field.

Acknowledgments This work was supported by the National Magnetic Confinement Fusion Science Program (Grant No. 2011GB112001), the Program of International S&T Cooperation (Grant No. 2013DFA 51050), the National Natural Science Foundation of China (Grant No. 11104224, 11004162, 51271155), the Research Fund for the Doctoral Program of Higher Education of China (Grant No. 20110184120029), the Fundamental Research Funds for the Central Universities (Grant No. 2682013ZT16, SWJTU11ZT31, 2682013CX004, SWJTU11BR063), and the Science Foundation of Sichuan Province (Grant No. 2011JY0031, 2011JY0130).

References

1. Kane CL, Mele EJ (2005) Z_2 topological order and the quantum spin Hall effect. Phys Rev Lett 95:146802
2. Bernevig BA, Zhang SC (2006) Quantum spin Hall effect. Phys Rev Lett 96:106802
3. Qu DX, Hor YS, Cava RJ (2012) Quantum oscillations in magnetothermopower measurements of the topological insulator Bi_2Te_3. Phys Rev Lett 109:246602
4. Wang J, Chang CZ, Li HD et al (2012) Interplay between topological insulators and superconductors. Phys Rev B 85:045415
5. Bernevig BA, Hughes TL, Zhang SC (2006) Quantum spin Hall effect and topological phase transition in HgTe quantum wells. Science 314:1757
6. Kong DS, Chen YL, Cha JJ, Zhang QF et al (2011) Ambipolar field effect in the ternary topological insulator $(Bi_xSb_{1-x})_2Te_3$ by composition tuning. Nat Nanotechnol 6:705–709
7. Scherrer H, Scherrer S (1996) In: Rowe DM (ed) Handbook of thermoelectrics. CRC Press, New York, pp 211–237
8. Hor YS, Richardella A, Roushan P et al (2009) P-type Bi_2Se_3 for topological insulator and low-temperature thermoelectric applications. Phys Rev B 79:195208
9. Qi XL, Hughes TL, Zhang SC (2008) Topological field theory of time-reversal invariant insulators. Phys Rev B 78:195424
10. Hsieh D, Qian D, Wray L et al (2008) A topological Dirac insulator in a quantum spin Hall phase. Nature 45:970–974
11. Zhang HJ, Liu CX, Qi XL et al (2009) Topological insulators in Bi_2Se_3, Bi_2Te_3 and Sb_2Te_3 with a single Dirac cone on the surface. Nat Phys 5:438–442
12. Chen YL, Analytis JG, Chu JH et al (2009) Experimental realization of a three-dimensional topological insulator Bi_2Te_3. Science 325:178–181
13. Hsieh D, Xia Y, Qian D et al (2009) Observation of time-reversal-protected single-Dirac-cone topological-insulator states in Bi_2Te_3 and Sb_2Te_3. Phys Rev Lett 103:146401
14. Wang ZH, Qiu RLJ, Lee CH et al (2013) Ambipolar surface conduction in ternary topological insulator $Bi_2(Te_{1-x}Se_x)_3$ nanoribbons. ACS Nano 7(3):2126–2131
15. Ni HL, Zhao XB (2007) Synthesization and properties of Bi_2Te_3 based nanocomposite thermoelectric materials. Zhejiang University
16. Kim TS, Kim IS, Kim TK et al (2002) Thermoelectric properties of p-type 25% Bi_2Te_3+75%Sb_2Te_3 alloys manufactured by rapid solidification and hot pressing. Mater Sci Eng B 90:42–46
17. Keawprak N, Sun ZM, Hashimoto H et al (2005) Effect of sintering temperature on thermoelectric properties of pulse discharge sintered $(Bi_{0.24}Sb_{0.76})(2)Te_3$ alloy. J Alloy Compd 397:236–244
18. Seo J, Lee C, Park K (1998) Effect of extrusion temperature and dopant on thermoelectric properties for hot-extruded p-type Te-doped $Bi_{0.5}Sb_{1.5}Te_3$ and n-type SbI_3-doped $Bi_2Te_{2.85}Se_{0.15}$. Mater Sci Eng B 54:135–140
19. Zhang HT, Luo XG, Wang CH et al (2004) Characterization of nanocrystalline bismuth telluride (Bi_2Te_3) synthesized by a hydrothermal method. J Cryst Growth 265:558–562
20. National Bureau of Standards (US) Monograph 25 (1964) Sec 3, 16